El-Feky and El-Rashedy
Beni-Suef Univ J Basic Appl Sci (2023) 12:108
https://doi.org/10.1186/s43088-023-00445-x

Beni-Suef University Journal of Basic and Applied Sciences

RESEARCH

Open Access

Sterols and flavonoids in strawberry calyx with free radical scavenging, anti-inflammatory, and molecular dynamic study

Amal M. El-Feky[1*] and Ahmed A. El-Rashedy[2]

Abstract

Background The phytochemical constitution and biological capabilities of *Fragaria ananassa*'s calyx have not been extensively investigated before. Consequently, the research study pointed for characterization, isolation, and identification of the sterols and flavonoids as the major active constituents in the calyx of *F. ananassa* and evaluation for their impacts as free radicals scavenger and anti-inflammatory agent.

Results GC/MS investigation for the lipoidal constitutions of *F. ananassa*'s calyx was performed to identify twenty-six compounds signifying 83.08%, as well as isolation of campesterol, stigmast-4-en-3-one, and β-sitosterol-D-glucoside by column chromatography technique. Additionally, quantification and identification of the flavonoids in the ethyl acetate extract was carried out by HPLC/DAD technique beside to isolation and structure elucidation of 5-hydroxy-7, 4′-dimethoxy flavone and Chrysin. The free radicals scavenging and anti-inflammatory activities of both non-polar and polar extracts have been tested against (DPPH and ABTS radicals) and (COX-1, COX-2, and 5-LOX enzymes), correspondingly. The results illustrated significant effects of the polar extract of *F. ananassa* calyx greater than non-polar one. The dynamic natures, binding interactions, and protein–ligand stabilities have also been investigated using the molecular dynamics (MD) simulation research. The MD simulation revealed that Chrysin's chromen ring was extended to catalytic position of COX-1 receptor, producing Pi-Pi T-shaped contact with Tyr 354 and Trp 356. In addition, Chrysin's chromen ring has formed a Pi-alkyl bond with Val 318 and Leu 321. However, due to the huge size of β-sitosterol-D-glucoside, the glycoside ring can form a hydrogen bond with Tyr 317. The cyclopentyl phenanthrene ring also possesses Pi-alkyl interactions with Ile 58, Leu 62, Val 85, Val 318, Tyr 324, Leu 326, Ala 496, and Leu 500.

Conclusions The findings of our study are crucial in establishing the molecular bases for Chrysin and β-sitosterol-D-glucoside action against anti-inflammatory targets and for developing more effective selective inhibitors. The discovery of the binding location for ATP can pave the door for development unique, structure-based approach for natural anti-inflammatory medications.

Keywords *Fragaria ananassa* calyx, Phytoconstituents, Antioxidant, Anti-inflammatory, Molecular docking

1 Background

Strawberry with Latin name *Fragaria ananassa* Duch., Rosaceae family, is popular and well-known fruit [1] that is have a large demand worldwide, not only for their flavoured taste but also for their health-related characteristics, as the fruits are acknowledged as a vital source of minerals, vitamins especially vitamin C and many phenolic compounds [2]. Many research studies

*Correspondence:
Amal M. El-Feky
ammelfeky@hotmail.com
[1] Pharmacognosy Department, National Research Centre, 33 El Bohouth St. (Former El Tahrir St.), Dokki, P.O. 12622, Giza, Egypt
[2] Natural and Microbial Products Department, National Research Center, 33 El Bohouth St. (Former El Tahrir St.), Dokki, P.O. 12622, Giza, Egypt

reported the major active constituents in fruits, leaves, and roots of *F. ananassa* as phenolics, tannins [3], flavonoids [4], beside to steroids, and triterpenoids [5]. The nutritious studies conducted that the long consumption of the strawberry fruits has a remarkable protecting effects against various chronic ailments such as Alzheimer, cancer [5], diabetes [6], and some cardiovascular diseases [7], beside to other health-promoting activities as free radical scavenging [3], anti-inflammatory [8], anti-obesity, and antiplatelet aggregation agent [9].

Around 60% of strawberry consumption was intended as fresh fruits, with the remaining 40% going primarily to frozen processing [10]. As a result, the processed fruits produce enormous amounts of calyx by-products. According to Villamil-Galindo et al. [11], strawberry by-products contain high concentration of phenolic compounds, producing industrial opportunities for getting raw materials at low cost with an intriguing additional value, perhaps lowering the cost of their eventual disposal.

Although *F. ananassa* fruit has been the subject of numerous studies, the calyx has received much less attention. For that reason, the current research study pointed to characterize, isolate, and identify the sterols and flavonoids as the principal active constituents presented in *F. ananassa* calyx, and evaluate their biological activities as free radical scavenging and anti-inflammatory agents.

2 Methods

2.1 Fruit collection and identification

Strawberry fruits have been gathered in June 2023 from private strawberry farm in El-Slaheya Elgdeda, Sharkia Governorate, Egypt. Taxonomical identity of the fruits was kindly confirmed by Prof. Dr. Gamal Farag, at the Ministry of Agriculture's Horticulture Research Centre. A specimen was deposited in the National Research Centre herbarium with Voucher number M183. Calyxes have been collected, cleaned, and dried by air before being powdered.

2.2 Extraction

Dried *F. ananassa* calyx powders (500 g) were defatted by extraction with petroleum ether (3L X 4 times) for lipoidal constituent extraction and after that the defatted powders were consequentially extracted with ethyl acetate (3L X 6 times) as polar solvent for flavonoids extraction, using cold maceration method. The lipoidal (yield 17%) and flavonoidal (yield 32%) portions have been concentrated at 45 °C by the rotavapour (Heidolph, Germany) and kept in refrigerator for chemical and biological investigation.

2.3 GC/MS investigation of the lipoidal constitutions

The lipoidal constitutions of *F. ananassa* calyx were investigated using GC/MS technique (Shimadzu GC/MS–QP5050A) using capillary column of fused silica, 30 m length, 0.53 mm ID and 1.5 µm thickness, and stationary phase DB-1 with mass detector. Temperature programming was adjusted to 50–150 °C at a rate of 10°C/min-250 °C(5 min), at 5 °C/min-270 (5 min), at 3.5°C/min, with ionization voltage 70 eV, and helium at 1 ml/min as carrier gas. Characterization was achieved through comparing the obtained fragments with that of the accessible recorded archives and reported literatures. Quantitative determination was performed according to peak area integration.

2.4 Isolation and structural elucidation of the major sterols

The major sterols presented in petroleum ether extract were isolated by using column chromatography technique, where five grams has been loaded on 175 g silica gel G60 for chromatographical adsorption analysis (BDH, England) in the column (140 × 3 cm). Eluting with petroleum ether and increasing the polarity with chloroform, each collected fraction (50 ml) was separately concentrated and detected for sterols existence through applying Liebermann–Burchard test. The fractions that responded positively have been purified by readymade chromatographic plates (20 × 20 cm) coated with silica gel (F-254, Fluka), with toluene:ethyl acetate (8:2 v/v). Visualization was performed at 365- and 254-nm UV wavelengths. After that, spraying was made by *p*-anisaldehyde-sulphuric acid and heated for 5 min at 105 °C; the same responded portions were mixed and concentrated. Structural elucidations of the pure isolated compounds were performed by melting points measurement and by different spectroscopic analyses (mass spectrometry, ^{1}H-NMR, and ^{13}C-NMR).

2.5 Quantitative estimation of flavones and flavonols

Quantification of flavones and flavonols has been done according to Bahloul et al. [12]. In brief, 1 mL from ethyl acetate extract has been added to 1 mL of 2% $AlCl_3$-ethanol solution. At 420 nm, absorbance was measured after a reaction had placed for 1 h at room temperature. To create the calibration curves, rutin (Fluka Biochemika, Sigma-Aldrich) has been chosen as reference. The results were calculated as mg rutin equivalent/100 g extract as mean ± S.D.

2.6 Quantitative estimation of flavanones and dihydroflavonols

The content of flavanones and dihydroflavonols has been assessed in accordance with Bahloul et al. [12]. In a nutshell, 1 mL of the ethyl acetate extract was mixed with 1 mL from a solution containing 1 g of 2,4-dinitrophenylhydrazine in 2 mL conc. sulphuric acid, and dilution by methanol to 100 mL, then heating was carried out for 1 h at 45 °C, then the mixture has been diluted by 10% alcoholic KOH to reach 10 mL. One millilitre from the obtained mixture has been added to 10 mL of methanol to make a 50-mL final volume. At 486 nm, absorbance was measured and data were displayed as mg naringenin equivalent in 100 g extract as mean ± S.D.

2.7 Identification of the flavonoids by HPLC/DAD technique

Identification of the flavonoids was carried out by high-performance liquid chromatography (HPLC) using Agilent Technologies 1100 series liquid chromatograph coupled with an autosampler and a diode-array detector [13].

2.8 Isolation and structure elucidation of flavonoids

Ethyl acetate extract of *F. ananassa* calyx (2 g) was applied on preparative TLC (20 × 20cm, Merck) using a developing system with dichloromethane:ethyl acetate (5:1) ratio. The bands that turned yellow when treated with ammonia and the $AlCl_3$ spray reagent [14] were marked, scratched off, and then collected after inspection via UV-254 and 365 nm. Several spectroscopic studies were used to identify the isolated flavonoids, along with comparisons to published data.

2.9 Free radicals scavenging effect

The free radicals scavenging effect of lipoidal and flavonoidal extracts of *F. ananassa* calyx at different concentrations of 0.01, 0.05, 0.1 mg was evaluated against 1,1-diphenyl-2-picryl-hydrazyl (DPPH) (Aldrich Chemie, Germany) and 2,2′-azinobis-(3-ethylbenzothiazoline-6-sulfonic acid) (ABTS) (Fluka Biochemika, Sigma-Aldrich) radicals using the techniques reported by Rahman et al. [15] and Arnao et al. [16], respectively. The method was carried out in comparison with vitamin C as a standard antioxidant (Sigma, USA). Values are represented by mean ± SD of three replicates.

2.10 In vitro anti-inflammatory evaluation

In vitro anti-inflammatory evaluation of the lipoidal and flavonoidal extracts of *F. ananassa* calyx was performed through inhibition of two isoenzymes cyclooxygenase COX-1 and COX-2 (ovine/human), along with 5-LOX enzyme (human recombinant).

COX-1 and COX-2 inhibition assay has been performed by means of COX-1 and COX-2 kit (Cayman, No.: 560131) [17], where different known concentrations of the tested extracts were added separately to a mixture of 10 µL of COX-1 or COX-2 and 0.1 M HCl buffer, left for incubation at room temperature for 10 min. After that, 10µL of arachidonic acid, fifty µL HCl and Ellman's reagent have been added. The absorbance has been determined at UV-410 nm alongside blank; IC50 has been determined via linear regression.

5-Lipoxygenase inhibition assay was carried out by 5-LOX kit (No. 437996, Sigma-Aldrich) [18], where different concentrations of the tested extracts were added to 90 µL from 5-LOX, 100 µL of de chromogen, then 10 µL from arachidonic acid was added and shaken for 10 min, the absorbance has been determined at UV-490 nm compared to blank. IC50 has been calculated through linear regression.

2.11 Statistics

Statistical valuations of the tested parameters were performed using SPSS 9.05 (USA). The significant variances were examined using one-way analysis of variance (ANOVA) following by Co-state computer program.

2.12 System preparation: molecular docking

Cyclooxygenase-1 which was solved at resolution 2.70 Å has been produced through protein data bank having code 2OYU [19] and then was prepared using UCSF Chimera [20]. pH has been adjusted to 7.5 by PROPKA [21]. ChemBioDraw Ultra 12.1 has been performed to make 2D structure [22] that was optimized aiming to energy reduction by Avogadro software [23] using steepest descent technique as well as MMFF94 force field. Hydrogen atoms were eliminated using UCSF Chimaera [20] to get ready for docking.

Using AutoDock Vina [24], docking computations were carried out; Gasteiger partial charge [25] was assigned. AutoDock graphical user interface from MGL tools has been applied for describing atom kinds [26]. Grid box has been calculated using the grid parameters $x = -20.6819$, $y = 50.7675$, and $z = 11.1067$ for the dimension and $x = 10.00$, $y = 10.00$, and $z = 10.00$ for the centre grid, with exhaustiveness = 8. The Lamarckian genetic technique [27] has been performed for producing docked conformation with decreasing directive of the docking energy.

2.13 Molecular dynamic (MD) simulations

Molecular dynamic (MD) simulations have been used for studying the biological systems; it is possible to

investigate atomic and molecular motions that are not readily accessible using conventional techniques [28]. Conducting this model has offered an extensive understanding for biological system changes as conformation shifts as well as molecular interactions [28]. All systems' MD simulations have been carried out by AMBER 18 package's PMEMD engine's GPU version [29, 30].

2.14 Post-MD analysis

The trajectories that produced from MD simulations have been assessed by AMBER18 suite's CPPTRAJ [31] model. All graphs and visualisations were made using Chimaera [20] and the Origin data analysis programme [32].

2.15 Thermodynamic calculations

For estimating ligand-binding affinities, the Poisson-Boltzmann or generalised Born and surface area continuum solvation (MM/PBSA and MM/GBSA) technique was reported as effective method [33–35]. The protein–ligand complex molecular simulations compute rigorous statistical–mechanical binding free energy within a defined force field [29, 30].

3 Results

3.1 GC/MS investigation of the lipoidal constitutions

GC/MS analysis was performed to pinpoint the lipoidal constituents in the non-polar extract of *F. ananassa* calyx. The identified compounds are illustrated in Table 1. Twenty-six compounds were identified signifying 83.08%, and constituting of 8 hydrocarbons (27.45%), 7 fatty alcohols (31.51%), 1 ketone (1.57%), 3 fatty acids (14.77%), 3 fatty acid esters (4.97%), and 4 sterols (2.81%). Interestingly, 9,12,15-octadecatrien-1-ol in addition to *n*-hexadecanoic acid was detected as major identified constituents amounting 11.59% and 9.42%, respectively. Campesterol,

Table 1 GC/MS investigation of the lipoidal constitutions in *F. ananassa* calyx

Class	Peak No	Compound	Rt (min.)	Molecular formula	Molecular weight	Base peak	Relative area %	Total concentration (%)
Hydrocarbon	1	*n*-Dodecane	5.32	$C_{12}H_{26}$	170	57	1.57	27.45
	2	*n*-Tetradecane	5.90	$C_{14}H_{30}$	198	57	4.26	
	3	Hexadecane	8.40	$C_{16}H_{34}$	226	57	4.78	
	4	Octadecane	11.71	$C_{18}H_{38}$	254	57	3.74	
	5	Nonadecane	13.54	$C_{19}H_{40}$	268	57	3.51	
	6	Eicosane	16.54	$C_{20}H_{42}$	282	57	1.78	
	7	*n*-Docosane	23.47	$C_{22}H_{46}$	310	57	4.85	
	8	*n*-Tricosane	25.82	$C_{23}H_{48}$	324	57	2.96	
Fatty alcohol	9	3-Methylbut-3-en-2-ol	13.96	$C_6H_{12}O$	100	41	1.89	31.51
	10	5-Methyl-1-heptanol	14.09	$C_8H_{18}O$	130	55	6.73	
	11	8-Dodecen-1-ol	22.95	$C_{12}H_{24}O$	184	55	1.25	
	12	3,7,11-Trimethyl-1,6,10-dodecatrien-3-ol	23.47	$C_{15}H_{26}O$	222	41	5.83	
	13	9,12,15-Octadecatrien-1-ol	26.71	$C_{18}H_{32}O$	264	41	11.59	
	14	Heneicosanol	28.01	$C_{21}H_{44}O$	312	55	2.14	
	15	1-Pentacosanol	29.33	$C_{25}H_{52}O$	368	55	2.08	
Ketone	16	6,10,14-Trimethyl-2-pentadecanone	25.80	$C_{18}H_{36}O$	268	43	1.57	1.57
Fatty acid	17	1,2-Benzenedicarboxylic acid	30.75	$C_8H_6O_4$	166	104	3.51	14.77
	18	*n*-Hexadecanoic acid	41.33	$C_{16}H_{32}O_2$	256	43	9.42	
	19	Octadecanoic acid	43.10	$C_{18}H_{36}O_2$	284	43	1.84	
Fatty acid ester	20	Hexadecanoic acid, methyl ester	32.11	$C_{17}H_{34}O_2$	270	74	2.37	4.97
	21	Hexadecanoic acid, ethyl ester	42.53	$C_{18}H_{36}O_2$	284	88	1.53	
	22	Docosanoic acid, ethyl ester	44.80	$C_{24}H_{48}O_2$	368	88	1.07	
Sterol	23	Campesterol	47.10	$C_{28}H_{48}O$	400	43	0.49	2.81
	24	Stigmasterol	50.11	$C_{29}H_{48}O$	412	55	0.61	
	25	β-Sitosterol	52.91	$C_{29}H_{50}O$	414	43	1.03	
	26	β-Sitosterol acetate	54.23	$C_{31}H_{52}O_2$	456	43	0.68	

stigmasterol, β-sitosterol beside to β-sitosterol acetate have been identified with concentration of 0.49%, 0.61%, 1.03%, and 0.68%, respectively. GC/MS chromatogram of the petroleum ether extract of *F. ananassa* calyx was illustrated in Additional file 1: Fig. S1.

3.2 Isolation and structural elucidation of the major sterols

Silica gel column chromatographic technique was performed for isolation of the sterols in the non-polar extract of *F. ananassa* calyx that produce purplish colour after spraying with *p*-anisaldehyde-sulphuric acid. Structure of isolated sterols has been established through melting points and by mass fragmentation pattern, ^{1}H-NMR, ^{13}C-NMR analyses as well as referring to previous findings.

Campesterol was isolated from the column by using petroleum ether: chloroform (95:5) as eluent and showed R_f 0.75 in silica gel TLC (F-254, Fluka) with toluene:ethyl acetate (8:2 v/v). The whitish crystal had m.p. 157 °C that was matching with Choi et al. [36]. EI-MS m/z (relative intensity) displayed molecular weight 400 (18%) for molecular formula $C_{28}H_{48}O$, base peak with m/z 129 (100%), besides m/z 43 (67%), 55 (49%), 69 (34), 81 (43), 119 (25), 145 (29), 161 (30), 213 (35), 231 (28), 255 (34), 289 (25), 315 (37), 367 (41), 382 (19). ^{1}H NMR (400 MHz, DMSO, δ ppm): 5.23 (1 olefinic H, m, H-6), 3.41 (1H, dd, H-3), 2.19 (1H, d, H-4), 1.12 (3H, s, H-19), 0.94 (1H, d, H-21), 0.82 (3H, d, H-27), 0.79 (3H, d, H-26), 0.75 (3H, d, H-28), and 0.64 (3H, s, H-18). ^{13}C-NMR (125 MHz, DMSO, δ ppm): 38.2 (C-1), 29.0 (C-2), 72.4 (C-3), 40.5 (C-4), 141.3 (C-5), 122.4 (C-6), 32.1 (C-7), 29.7 (C-8), 51.3 (C-9), 37.1 (C-10), 19.8 (C-11), 39.5 (C-12), 40.1 (C-13), 57.2 (C-14), 22.3 (C-15), 27.5 (C-16), 55.6 (C-17), 20.4 (C-18), 15.3 (C-19), 31.8 (C-20), 19.2 (C21), 34.6 (C-22), 22.6 (C-23), 41.6 (C-24), 36.5 (C-25), 17.6 (C-26), 18.4 (C-27), 23.7 (C-28). The data spectral values for campesterol agreed with those reported in the literature [37, 38].

Stigmast-4-en-3-one was isolated by using petroleum ether: chloroform (85:15) as white needles, R_f 0.78, m.p. 154 °C which in agreement with [39], EI-MS m/z (relative intensity) displays molecular weight 412 (18%) for molecular formula $C_{29}H_{48}O$. Distinctive fragments were 43 (46%), 55 (38%), 71 (35%), 95 (31%), 124 (100%), 178 (22%), 213 (26%), 229 (32%), 255 (27%), 329 (19%), 381 (36%), 396 (46%). ^{1}H NMR (400 MHz, DMSO, δ ppm): 5.51 (1 olefinic H, m, H-4), 3.6 (2H, d,H-22), 3.7 (2H, d,H-23), 1.7 (3H, s, H-19), 0.95 (3H, s, H-29), 7.3 (1H,d, H-24), 11.0 (1H,d, H-25). ^{13}C-NMR (125 MHz, DMSO, δ ppm): 36.4 (C-1), 34.2 (C-2), 170.1 (C-3), 122.6 (C-4), 197.1 (C-5), 32.8 (C-6), 32.0 (C-7), 36.0 (C-8), 52.8 (C-9), 38.9 (C-10), 19.9 (C-11), 40.1 (C-12), 41.6 (C-13), 56.4 (C-14), 23.5 (C-15), 27.7 (C-16), 56.2 (C-17), 11.8 (C-18), 16.8 (C-19), 35.6 (C-20), 18.0 (C21), 32.7 (C-22), 24.5 (C-23), 44.6 (C-24), 23.1 (C-25), 19.5 (C-26), 18.2 (C-27), 22.9 (C-28), 11.38 (C-29), which is accordant with Udobre et al. [40].

β-Sitosterol-D-glucoside was isolated by using petroleum ether: chloroform (80:20) and by further purification on preparative silica gel TLC using toluene: ethyl acetate (9:1) as a developing solvent giving blue band with R_f 0.70 which converted to purple colour by vanillin-sulphuric acid treating. The isolated compound was purified as white crystals, m.p. 280 °C which in harmony with that reported by Aboulthana et al. [41]. EI-MS m/z (relative intensity) illustrated molecular weight 576 (24%) for molecular formula $C_{35}H_{60}O_6$, base peak for 57, beside to 414 (65%) assigned to β-sitosterol moiety, 396 (35%), 381 (28%), 329 (19%), 303 (25%), and 275 (27%). ^{13}CNMR: δ ppm 10.9 (C-18), 10.3 (C-29), 19.8 (C-21), 19.2 (C-27), 18.7 (C-19), 18.4 (C-26), 19.6 (C-11), 22.1 (C-28), 24.7 (C-15), 25.8 (C-23), 28.3 (C-16), 27.6 (C-2), 28.8 (C-25), 29.9 (C-7/8), 34.2 (C-22), 36.6 (C-20), 35.9 (C-10), 35.4 (C-1), 38.2 (C-4), 40.1 (C-12), 43.2 (C-13), 45.4 (C-24), 48.6 (C-9), 54.7 (C-17), 55.1 (C-14), 60.2 (C-6′), 72.3 (C-4′), 74.2 (C-2′), 77.8 (C-3), 78.1 (C-3′/5′), 99.3 (C-1′), 120.7 (C-6), 139.2 (C-5). The obtained results were in consistence with Horník et al. [42].

3.3 Quantitative estimation of the flavonoids

The contents of flavones and flavonols were determined in the ethyl acetate extract of *F. ananassa* calyx as 3157.6 ± 0.16 mg rutin equivalent /100 g extract. However, flavanones and dihydroflavonols were provided at significantly lower concentration as 281.4 ± 0.09 mg naringenin equivalent/100 g extract.

3.4 Identification of the flavonoids by HPLC/DAD technique

HPLC/DAD technique was applied to quantitatively and qualitatively investigate the flavonoids composition in the ethyl acetate extract of *F. ananassa* calyx, as indicated in Table 2. Nineteen flavonoids were identified using the HPLC/DAD study. The three main detected flavonoids were revealed to be quercetin (2491.36 mg/100 g), apigenin (1638.48 mg/100 g), as well as kaempferol (1467.29 mg/100 g). HPLC chromatogram of the ethyl acetate extract of *F. ananassa* calyx was provided in Additional file 1: Fig. S2.

3.5 Isolation and structure elucidation of the principal flavonoids

5-Hydroxy-7, 4′-dimethoxy flavone was isolated as yellowish crystals, m.p.255 °C. It produced a yellow colour under short UV light, but after being exposed to ammonia and $AlCl_3$ spray reagent with R_f of 0.65, it fluoresced

Table 2 HPLC investigation of the flavonoids in the polar extract of *F. ananassa* calyx

Flavonoids	Concentration (mg/100 g)
Apigenin	1638.48
Apigenin-7-glucoside	314.85
Apigenin-7-O-neohespiroside	286.04
Kaempferol	1467.29
Kaempferol-3-O-rutinoside	160.58
Kaempferol-3-rhamnoside	117.36
Quercetin	2491.36
Quercitrin	291.34
Rutin	183.76
Rhamnetin	95.78
Isorhamnetin-3-Oglucoside	64.82
Luteolin	942.75
Luteolin-7-O-glucoside	103.58
Hesperidin	68.49
Hesperetin	173.61
Naringenin	198.42
Naringin	81.35
Myricetin	924.71
Chrysoeriol	739.65

intensely yellow. ^{1}H NMR (400 MHz, DMSO, δ ppm): 5.60 (1H, s, H-3), 6.52 (1H, d, H-6), 6.43 (1H, d, H-8), 7.86 (2H, dd, H-2′, H-6′), 7.88 (2H, dd, H-3′, H-5′), 3.86 (3H, s, OCH3). ^{13}C-NMR (125 MHz, DMSO, δ ppm): 129.3 (C-2), 99.4 (C-3), 183.5 (C-4), 161.0 (C-5), 100.3 (C-6), 163.8 (C-7), 91.4 (C-8), 160.5 (C-9), 103.1 (C-10), 119.6 (C-1′), 128.1 (C-2′), 135.6 (C-3′), 146.1 (C-4′), 135.8 (C-5′), 128.3 (C-6′), 54.7 (OCH_3). The obtained spectral data harmonized to the previously reported literature [43].

Chrysin (5,7-dihydroxy flavone) was isolated as yellow crystals, m.p.285 °C, produced yellowish colour with short UV light converted to intense yellowish fluorescence after exposure to ammonia and $AlCl_3$ spray reagent with R_f 0.78, ^{1}H NMR (400 MHz, DMSO, δ ppm): 6.25 (1H, d, H-6), 6.43 (1H, d, H-8), 6.98 (1H, s, H-3), 7.49 (1H, m, H-4′), 7.93 (2H, dd, H-2′, H-6′), 8.04 (2H, dd, H-3′, H-5′). ^{13}C-NMR (125 MHz, DMSO, δ ppm): 163. 6 (C-2), 102.3 (C-3), 180.2 (C-4), 160.8 (C-5), 98.7 (C-6), 163.9 (C-7), 93.7 (C-8), 158.4 (C-9), 103.9 (C-10), 129.5 (C-1′), 127.4 (C-2′), 128.5 (C-3′), 138.4 (C-4′), 128.6 (C-5′),127.5 (C-6′). The spectroscopic results matched to that stated by Shrestha et al. [44].

3.6 Free radicals scavenging effect

By scavenging harmful free radicals, the antioxidants have been proposed to be important agents to protect cells from damage. It is noteworthy that continuous consumption of various antioxidant-rich vegetables is linked to a lower risk for developing many chronic diseases [12].

The free radicals scavenging capabilities of the non-polar and polar extracts of *F. ananassa* calyx against DPPH and ABTS radicals were determined in serial concentrations (0.01, 0.05, 0.1 mg), and it was observed that the lipoidal constitutions scavenged the DPPH free radicals by 53%, 68%, and 84% and ABTS by 29%, 59%, 83% at concentrations of 0.01, 0.05, and 0.1 mg, correspondingly. However, the flavonoidal constitutions recorded DPPH inhibition by 57%, 73%, 89% and ABTS inhibition by 36%, 61%, 84% at 0.01, 0.05, and 0.1 mg, respectively, as illustrated in Table 3. The obtained results revealed concentration-dependent radicals scavenging effects of both non-polar and polar extracts of *F. ananassa* calyx; these findings were supported by the identification of numerous active constituents (sterols and flavonoids, respectively) that have the antioxidant capacity.

3.7 In vitro anti-inflammatory effect

Cyclooxygenases (COX-1 and COX-2) beside to lipoxygenase (5-LOX) are well-known pro-inflammatory enzymes, and they are essential enzymes for arachidonic acid synthesis [45]. Therefore, these enzymes are frequently employed for screening and evaluation of the anti-inflammatory agents. Additionally, 5-lipoxygenase (5-LOX) promotes the second major metabolic path

Table 3 Free radicals scavenging effects of non-polar and polar extracts of *F. ananassa* calyx against DPPH and ABTS

Tested groups	Inhibition percentages (%)					
	DPPH			ABTS		
	0.01 mg/mL	0.05 mg/mL	0.1 mg/mL	0.01 mg/mL	0.05 mg/mL	0.1 mg/mL
Petroleum ether extract	53 ± 0.31	68 ± 0.09	84 ± 0.05	29 ± 0.20	59 ± 0.17	83 ± 0.11
Ethyl acetate extract	57 ± 0.20	73 ± 0.18	89 ± 0.23	36 ± 0.13	61 ± 0.14	84 ± 0.07
Vitamin C	62 ± 0.17	79 ± 0.21	94 ± 0.19	37 ± 0.07	68 ± 0.11	89 ± 0.05

Values are represented by mean ± SE of three replicates

to release eicosanoids. Leukotriene B4 is the last product of the 5-LOX pathway and is a mediator for a number of inflammations and sensitized diseases. Therefore, lowering leukotriene levels through 5-LOX inhibition could help in minimizing the risk of cardiovascular and gastrointestinal problems [46]. Because of the various side effects and limited activities of the synthetic drugs, search for natural anti-inflammatory agents is essential since they could be safer and more effective than the synthetic medicines [47].

The efficacy of non-polar and polar extracts of *F. ananassa* calyx to prohibit COX-1, COX-2, and 5-LOX enzymes was used for evaluation of their anti-inflammatory activities. According to Table 4, the ethyl acetate extract significantly inhibited COX-1 and COX-2 by IC50 = 0.428 ± 0.08 ug/mL and IC50 = 0.695 ± 0.14 ug/mL, respectively. In comparison with indomethacin standard (IC50 = 0.361 ± 0.13 ug/mL and 0.628 ± 0.11 ug/mL), as well as significantly prohibited the 5-LOX enzyme by IC50 = 0.501 ± 0.10 ug/mL compared with Zileuton (IC50 = 0.425 ± 0.09 ug/mL), while the petroleum ether extract showed less notable inhibition to COX-1, COX-2, and 5-LOX enzymes (IC50 = 0.613 ± 0.19, 1.062 ± 0.20 &0.731 ± 0.08) ug/mL, respectively (Fig. 1). Sterols and flavonoids present in the polar and non-polar extracts have several advantageous biological functions [48–50]. Flavonoids' capabilities are influenced by number of OH groups, conjugations, and resonances [51, 52], while sterols' impacts depend on saturation degree as well as side-chain length in their structure [53].

Table 4 IC50 values of non-polar and polar extracts of *F. ananassa* calyx against COX-1, COX-2 and 5-LOX

Tested group	IC50 values (ug/mL)		
	COX-1	COX-2	5-LOX
Petroleum ether extract	0.613 ± 0.19	1.062 ± 0.20	0.731 ± 0.08
Ethyl acetate extract	0.428 ± 0.08	0.695 ± 0.14	0.501 ± 0.10
Indomethacin	0.361 ± 0.13	0.628 ± 0.11	
Zileuton			0.425 ± 0.09

Assays were run in threefold ($n = 3$), and the results were presented by mean ± SE

3.8 Molecular dynamic and system stability

The molecular dynamic simulation has been conducted for forecasting how the isolated compound could behave when it bound with the protein's site as well as its interacting and stabilization [29, 30]. System's stability has been assessed via root-mean-square deviation (RMSD) in simulations of 20 ns. The determined RMSD data for the frames of apo-protein, Chrysin-complex, and β-sitosterol-D-glucoside-complex system were 1.86 ± 0.33 Å, 1.74 ± 0.20 Å, and 1.66 ± 0.34 Å, respectively (Fig. 2A). These findings demonstrated that β-sitosterol-D-glucoside binded to the protein complex system in considerably higher firm configuration compared to the other compounds under study.

Through MD simulation, assessment of the flexibility of the protein structure after ligand interaction is important in examination of the behavioural characters of the residue and its connection with the ligand [54]. Using the root-mean-square fluctuation (RMSF)

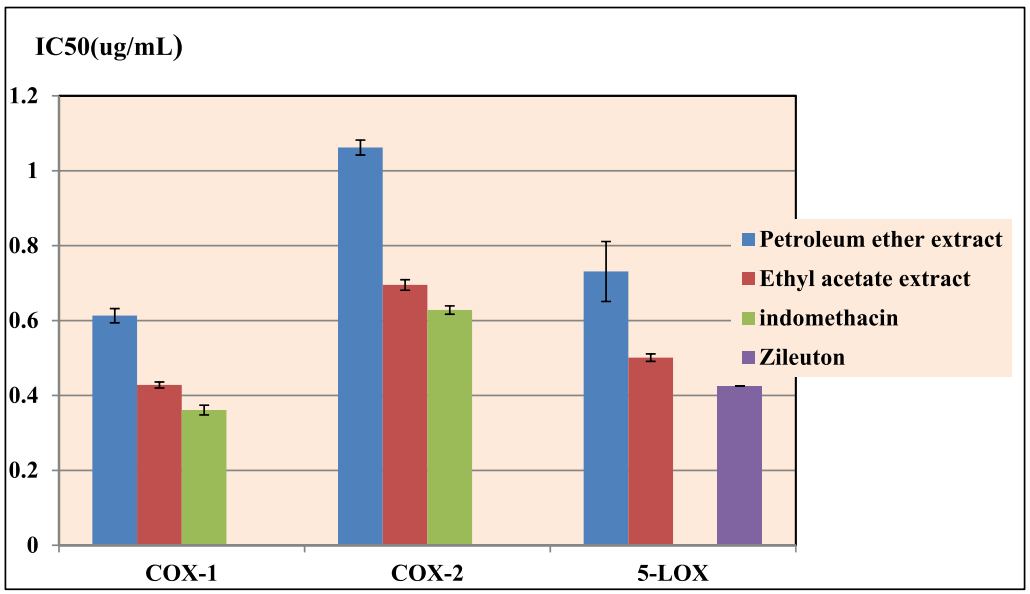

Fig. 1 IC50 values of non-polar and polar extracts of *F. ananassa* calyx against COX-1, COX-2 and 5-LOX

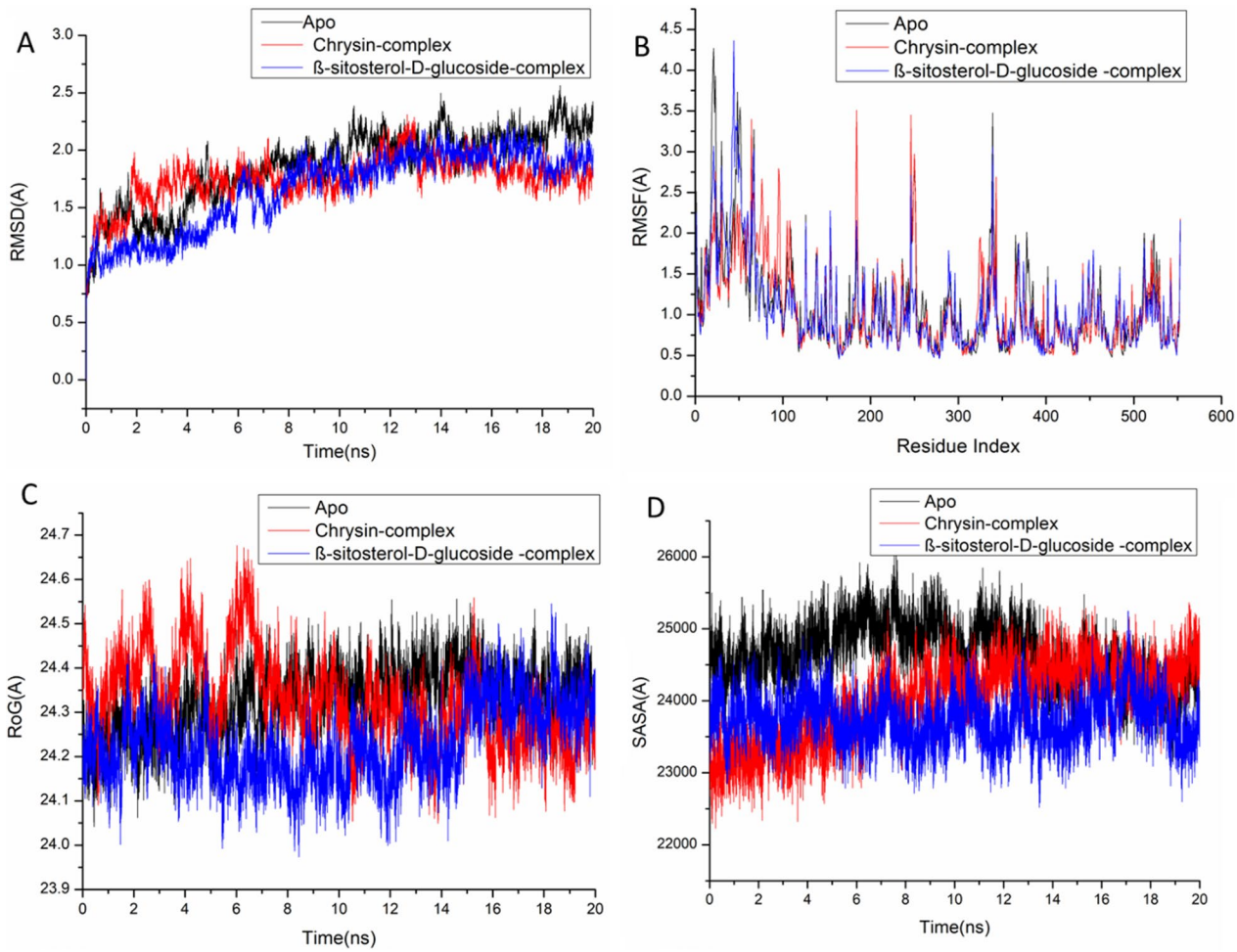

Fig. 2 **A** RMSD of Cα atoms of the protein backbone atoms. **B** RMSF of each residue of the protein backbone Cα atoms of protein residues **C** ROG of Cα atoms of protein residues; **D** solvent-accessible surface area (SASA) of the C α of the backbone atoms relative (black) to the starting minimized over 20 ns for the catalytic binding site with Chrysin-complex system (red),and β-sitosterol-D-glucoside (blue)

technique, protein residue variations have been determined for defining the influence of inhibitor binding to the relevant target through 20-ns simulations. The calculated RMSF data 1.1182 ± 0.59 Å, 1.085 ± 0.52 Å, and 1.066 ± 0.55 Å for systems apo-protein, Chrysin-complex, and β-sitosterol-D-glucoside complex systems, respectively. Figure 2B depicts the overall residue fluctuations of the compounds. These findings demonstrated that β-sitosterol-D-glucoside bonded to protein complex system with less residual fluctuations compared to other tested compounds.

ROG was considered for estimating the whole system's compaction and stabilization after ligand bounding through MD simulations [55, 56]. The Rog data for apo-protein, Chrysin-complex, and β-sitosterol-D-glucoside -complex systems were 24.32 ± 0.07 Å, 24.32 ± 0.099 Å, and 24.22 ± 0.084 Å, correspondingly (Fig. 2C). According to the noticed characteristics, β-sitosterol-D-glucoside-bounded complex has an extremely strong structure against the catalytic-bounding position in COX-1 receptor.

Protein's solvent-accessible surface area (SASA) was determined to assess the compact for protein's hydrophobic core. This has been accomplished via measuring protein's solvent-visible surface area, that is crucial in long-term biomolecules stabilization [57]. The SASA findings for apo-protein, Chrysin-complex, and β-sitosterol-D-glucoside-complex systems were 24,630 Å, 24,004.66 Å, and 23,743 Å, respectively (Fig. 2D). After reviewing the SASA results with RMSD, RMSF, and ROG computation data, it was established that β-sitosterol-D-glucoside complex system persists intact inside the COX1 receptor's catalytic binding position.

Table 5 Calculated energy binding for the compound against the catalytic binding site receptor of COX-1 receptor

Energy components (kcal/mol)					
Complex	**ΔE_{vdW}**	**ΔE_{elec}**	**ΔG_{gas}**	**ΔG_{solv}**	**ΔG_{bind}**
Chrysin	− 38.57 ± 0.12	− 19.82 ± 0.36	− 53.94 ± 0.51	19.88 ± 0.22	− 38.50 ± 0.16
β-Sitosterol-D-glucoside	− 75.712 ± 0.17	− 20.159 ± 0.419	− 95.87 ± 0.39	16.27 ± 0.19	− 79.59 ± 0.27

ΔE_{vdW} van der Waals energy, ΔE_{ele} electrostatic energy, ΔG_{solv} solvation free energy, ΔG_{bind} calculated total binding free energy

3.9 Binding interaction mechanism based on binding free energy calculation

The molecular mechanics energy approach (MM/GBSA) has been performed for figuring out the free bounding energies of tiny molecules to biological macromolecules that combines the generalized Born and surface area continuum solvation, and it could be extra accurate than docking scores [58]. The binding free energies have been assessed by MM/GBSA programme in AMBER18 by taking snapshot for systems' trajectories. As presented in Table 5, the whole determined energy components (with the exception of ΔG_{solv}) showed great negative results signifying promising interactions. The findings signposted that binding affinity of the Chrysin-complex and β-sitosterol-D-glucoside-complex were − 31.81 kcal/mol and − 40.80 kcal/mol, respectively.

The interaction of the ligand compound to COX-1 protein residue was regulated via greater positively van der Waals energy components, which demonstrated through comprehensive investigation for an individual energy contribution, resulting in described binding free energy. Significant binding free energy level was detected in the gas phase for all the inhibition process reaching values up to − 149.81kcal/mol (Table 5).

3.10 Identification of the critical residues responsible for ligands binding

From Fig. 3, Chrysin compound makes its greatest contribution to the COX-1 receptor's catalytic binding site which primarily detected from residues Tyr 317 (− 0.802 kcal/mol), Val 318 (− 1.06 kcal/mol), Leu321 (− 2.014 kcal/mol), Ser322 (− 1.083 kcal/mol), Tyr324 (− 0.331 kcal/mol), Phe350 (− 0.409 kcal/mol), Leu 353 (− 2.747 kcal/mol), Tyr 354 (− 1.177 kcal/mol), Trp356 (− 0.438 kcal/mol), Phe 487 (− 1.001 kcal/mol), Met491 (− 0.581 kcal/mol), Ile492 (− 1.814 kcal/mol), Met494 (− 0.366 kcal/mol), Gly495 (− 1.689 kcal/mol), Ala496 (− 1.89 kcal/mol), Ser 499 (− 1.486 kcal/mol), and Leu500 (− 0.216 kcal/mol).

However, the significant positive contribution of β-sitosterol-D-glucoside compound to the catalytic binding site of COX-1 receptor is primarily shown from residues Phe 57 (− 0.278 kcal/mol), Ile58 (− 1.92 kcal/mol), Leu61 (− 1.109 kcal/mol), Leu 62 (− 1.757 kcal/mol), Leu81 (− 0.923 kcal/mol), Met82 (− 0.749 kcal/mol), Leu 84 (− 1.986 kcal/mol) Val 85 (− 1.424 kcal/mol), Val 88 (− 1.496 kcal/mol), Arg89 (− 1.488 kcal/mol), Tyr317 (− 1.505 kcal/mol), Val 318 (− 2.444 kcal/mol), Leu321 (− 2.116 kcal/mol), Ser322 (− 1.072 kcal/mol), Tyr324 (− 0.474 kcal/mol), Leu326 (− 1.129 kcal/mol), Leu 328 (− 1.321 kcal/mol), Tyr 354 (− 0.911 kcal/mol), Trp356 (− 0.329kcal/mol), Phe 487 (− 0.653kcal/mol), Met491 (− 2.174 kcal/mol), Ile492 (− 2.26 kcal/mol), Glu 493 (− 0.261 kcal/mol), Gly495 (− 0.94 kcal/mol), Ala496 (− 1.67 kcal/mol), Ser 499 (− 1.546 kcal/mol), and Leu500 (− 1.492 kcal/mol). (Fig. 3). Validation of the docking performance and accuracy was illustrated in Additional file 1: Fig. S3. Autodocking vina docking results for Extracted compounds docked into the catalytic domain binding site in comparison to the co-crystallized IMS ligand was provided in Additional file 1: Table S1.

3.11 Ligand–residue interaction network profiles

The principal objective of drug design is making structure adjustment for the tested compounds in order to boost bioavailability, lower toxicity, and enhance pharmacokinetics [59]. COX-1 enzyme is found in the kidney, stomach, and platelets of humans [60] and stimulates the formation of thromboxanes, platelet aggregation, and vasoconstriction via promoting the eicosanoids generation [61, 62]. It should be highlighted that natural products have the potential to be both safer and more effective than manufactured drugs. Therefore, it is vitally necessary to develop novel natural products with the ability to inhibit the COX-1 enzyme. In this investigation, it was discovered that the structural interactions of both compounds in the catalytic binding site of the COX-1 receptor were hydrophobic and electrostatic.

Figure 4 illustrates Chrysin's chromen ring being extended into the catalytic active site and producing Pi-Pi T-shaped contact with Tyr 354 and Trp 356, respectively. Additionally, Chrysin's chromen ring has formed a Pi-alkyl connection with Val 318 and Leu 321. Nevertheless, because of the massive size of β-sitosterol-D-glucoside, the glycoside ring can form a hydrogen bonding connection with Tyr 317. Moreover, the cyclopentyl phenanthrene ring has established Pi-alkyl interactions with Ile

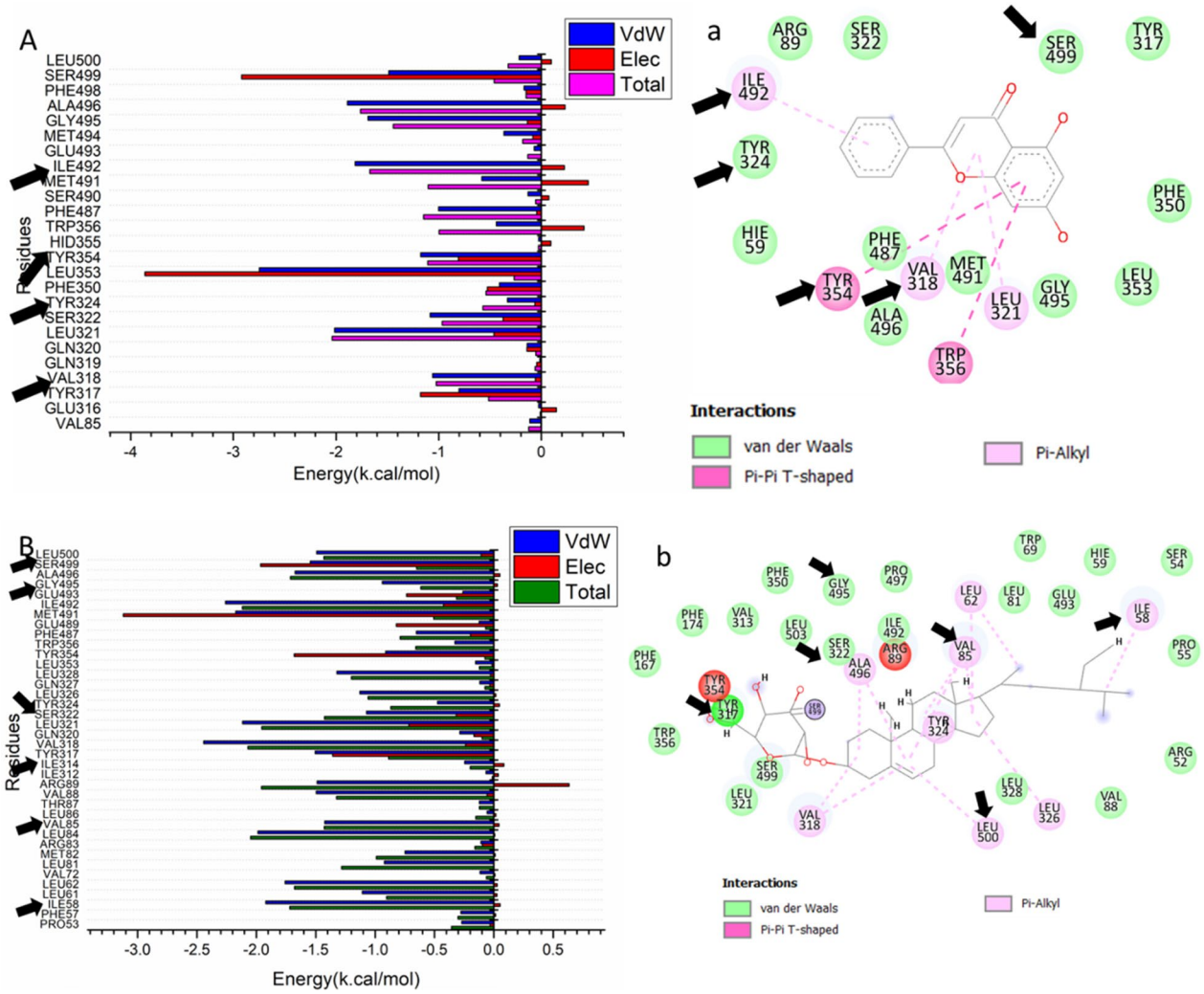

Fig. 3 Per-residue decomposition plots showing the energy contributions to the binding and stabilization of Chrysin (**A**) and β-sitosterol-D-glucoside (**B**) into catalytic binding site of COX-1 receptor, corresponding inter-molecular interactions are shown (**a**, **b**), while catalytic interaction residues are indicated in black arrow

58, Leu 62, Val 85, Val 318, Tyr 324, Leu 326, Ala 496, and Leu 500.

4 Discussion

A lot of effort has gone into researching natural antioxidants of plant origins [49, 50]. Due to a variety of steroidal and flavonoidal constituents in *F. ananassa* calyx, steroidal (non-polar) and flavonoidal (polar) extracts demonstrated considerable free radicals scavenging and anti-inflammatory impacts. The biological capabilities of flavonoids depend on their structure, whereas the flavonoids have fifteen carbons in the flavone skeleton (C6–C3–C6), comprising of double benzene rings (A and B) connected through pyran ring (C) [51]. It is worthily to mention that antioxidant effect of flavonoids is correlated to their chemical structures with numbers and locations of the OH groups, besides the conjugations and resonances [52].

As well as the structure of sterols affects their pharmacological actions, where their structures consist of a steroid skeleton with saturated connection of C-5 and C-6. Their biological activities are influenced by the hydroxyl group associated to the C-3 atom and the aliphatic side chain (saturation level and side-chain length) coupled to the C-17 atom in their chemical structures [53].

The molecular dynamic simulation has been conducted for forecasting how the isolated compound could behave when it bound with the protein's site as well as its interaction and stabilization [29, 30]; the results showed that chrysin and β-sitosterol-D-glucoside binded to the

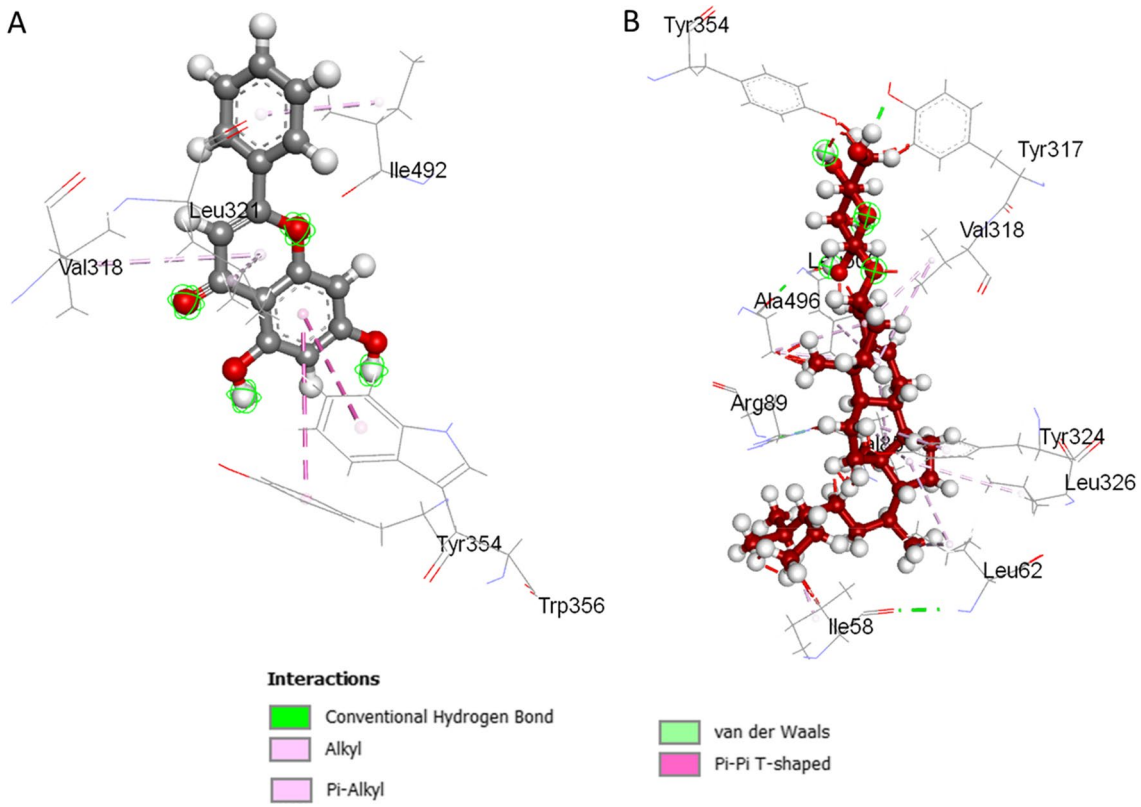

Fig. 4 The interaction residue of Chrysin (**A**) and β-sitosterol-D-glucoside (**B**) into the catalytic binding site of COX-1 receptor

protein complex system in considerably higher firm configuration and less residual fluctuation compared to the other compounds under study. Furthermore, after reviewing the SASA results with RMSD, RMSF, and ROG calculated data, it was found that the β-sitosterol-D-glucoside complex system exists in its entirety inside the COX1 receptor's catalytic binding site.

Additionally, MD simulation revealed that Chrysin's chromen ring was extended into the catalytic active site of COX-1 receptor, producing a Pi-Pi T-shaped contact with Tyr 354 and Trp 356. In addition, Chrysin's chromen ring has formed a Pi-alkyl bond with Val 318 and Leu 321. However, due to the huge size of β-sitosterol-D-glucoside, the glycoside ring can form a hydrogen bond with Tyr 317. The cyclopentyl phenanthrene ring also possesses Pi-alkyl interactions with Ile 58, Leu 62, Val 85, Val 318, Tyr 324, Leu 326, Ala 496, and Leu 500. In this investigation, it was discovered that the structural interactions of both compounds in the catalytic binding site of the COX-1 receptor were hydrophobic and electrostatic.

The binding affinity of the Chrysin-complex and β-sitosterol-D-glucoside-complex towards the COX-1 receptor was − 31.81 kcal/mol and − 40.80 kcal/mol, respectively. According to the binding free energy component analysis, the van der Waals energy component is the primary energy component driving this synergistic impact. The breakdown of total energies into cox-1 receptor active site residue contributions revealed that amino acid residues Tyr 317, Val 318, Leu321, Ser322, Tyr324, Phe350,Leu 353, Tyr 354,Trp356, Phe 487, Met491, Ile492,Met494, Gly495,Ala496, Ser 499,Leu500 are important in COX-1 receptor.

5 Conclusion

Petroleum ether and ethyl acetate extracts of *F. ananassa* calyx proved significant free radicals scavenging and anti-inflammatory impacts due to variety of steroidal and flavonoidal compounds having a number of pharmacological functions. After that, the interaction's stabilization has been evaluated utilizing the standard atomistic 20 ns dynamic simulation research. Various parameters from MD simulation trajectories have been estimated and confirmed for the protein–ligand complex's stabilization in dynamic settings. The selectivity mechanism of Chrysin and β-sitosterol-D-glucoside against COX-1 receptor has been examined by means of comparative MD simulation and binding free energy analysis. The findings of our

study are crucial in establishing the molecular bases for Chrysin and β-sitosterol-D-glucoside action against anti-inflammatory targets and for developing more effective selective inhibitors.

Abbreviations

F. ananassa	*Fragaria ananassa*
GC/MS	Gas chromatography/mass spectrometry
^{1}H-NMR	Proton nuclear magnetic resonance
^{13}C-NMR	Carbon nuclear magnetic resonance
HPLC/DAD	High-performance liquid chromatography with diode array
TLC	Thin-layer chromatography
UV	Ultraviolet
DPPH	1,1-Diphenyl-2-picryl-hydrazyl
ABTS	2,2′-Azinobis-(3-ethylbenzothiazoline-6-sulfonic acid)
COX	Cyclooxygenase
5-LOX	5-Lipoxygenase
HCl	Hydrochloric acid
IC50	Half maximal inhibitory concentration
MD	Molecular dynamic
PBSA	Poisson–Boltzmann and surface area continuum solvation
GBSA	Generalised Born and surface area continuum solvation
EI-MS	Electron ionization mass spectrometry
m.p.	Melting point
RMSD	Root-mean-square deviation
RMSF	Root-mean-square fluctuation
SASA	Solvent-accessible surface area
ROG	Radius of gyration
MM/GBSA	Molecular mechanics generalised Born and surface area
MM/PBSA	Molecular mechanics Poisson–Boltzmann and surface area
Phe	Phenylalanine
Ile	Isoleucine
Leu	Leucine
Met	Methionine
Val	Valine
Arg	Arginine
Ser	Serine
Tyr	Tyrosine
Gly	Glycine
Ala	Alanine

Supplementary Information

The online version contains supplementary material available at https://doi.org/10.1186/s43088-023-00445-x.

Additional file 1.. Supplementary file.

Acknowledgements
The scientific investigation has been achieved in the research laboratory in National Research Centre, Egypt.

Author contributions
AME-F helped in planning for the research subject, literature collection, conceptualization, phytochemical characterization, examination, revising the data, interpretation of the results, reviewing the work, writing the manuscript. AAE-R was involved in molecular dynamic study, calculation and computation, interpretation of the results, data analysis, writing.

Funding
There is no definite donation for this research from any funding organization.

Availability of data and materials
The study's supported data have been included in the manuscript as Additional file 1.

Declarations

Ethical approval and consent to participate
The research study has been carried out following the ethical guiding principles of the Medical Research Ethical Committee in National Research Centre, Egypt, with approval NO. 2447082023.

Consent for publication
Not applicable.

Competing interests
No conflicting interests to be reported.

Received: 3 August 2023 Accepted: 5 November 2023
Published online: 13 November 2023

References

1. El-Hawary SS, Mohammed R, El-Din ME, Hassan HM, Ali ZY, Rateb ME, Othman EM, Abdelmohsen UR (2021) Comparative phytochemical analysis of five Egyptian strawberry cultivars (Fragaria× ananassa Duch.) and antidiabetic potential of Festival and Red Merlin cultivars. RSC Adv 11(27):16755–16767
2. Giampieri F, Forbes-Hernandez TY, Gasparrini M, Alvarez-Suarez JM, Afrin S, Bompadre S et al (2015) Strawberry as a health promoter: an evidence based review. Food Funct 6(5):1386–1398
3. Aaby K, Ekeberg D, Skrede G (2007) Characterization of phenolic compounds in strawberry (Fragaria 9 ananassa) fruits by different HPLC detectors and contribution of individual compounds to total antioxidant capacity. J Agric Food Chem 55:4395–4406
4. Warner R, Wu BS, MacPherson S, Lefsrud M (2021) A review of strawberry photobiology and fruit flavonoids in controlled environments. Front Plant Sci 12:611893
5. Itoh T, Ninomiya M, Yasuda M, Koshikawa K, Deyashiki Y, Nozawa Y, Akao Y, Koketsu M (2009) Inhibitory effects of flavonoids isolated from Fragaria ananassa Duch on IgE-mediated degranulation in rat basophilic leukemia RBL-2H3. Bioorg Med Chem 17:5374–5379
6. Sheik Abdulazeez S (2014) Effects of freeze-dried Fragaria ananassa powder on alloxan-induced diabetic complications in Wistar rats. J Taibah Univ Med Sci 9:268–273
7. Miller K, Feucht W, Schmid M (2019) Bioactive compounds of strawberry and blueberry and their potential health effects based on human intervention studies: a brief overview. Nutrients 11:1–12
8. Van de Velde F, Esposito D, Grace MH, Pirovani ME, Lila MA (2019) Anti-inflammatory and wound healing properties of polyphenolic extracts from strawberry and blackberry fruits. Food Res Int 121:453–462
9. Parra-Palma C, Moya-León MA, Ramos P, Fuentes E, Palomo I, Torres CA (2018) Linking the platelet antiaggregation effect of different strawberries species with antioxidants: metabolomic and transcript profiling of polyphenols. Bol Latinoam Caribe Plant Med Aromat 17:36–52
10. Van de Velde F, Vaccari MC, Piagentini AM, Pirovani MÉ (2016) Optimization of strawberry disinfection by fogging of a mixture of peracetic acid and hydrogen peroxide based on microbial reduction, color and phytochemicals retention. Food Sci Technol Int 22(6):485–495
11. Villamil-Galindo E, Van de Velde F, Piagentini AM (2021) Strawberry agro-industrial by-products as a source of bioactive compounds: effect of cultivar on the phenolic profile and the antioxidant capacity. Bioresour Bioprocess 8(1):61
12. Bahloul N, Bellili S, Aazza S, Chérif A, Faleiro ML, Antunes MD, Miguel MG, Mnif W (2016) Aqueous extracts from tunisian diplotaxis: phenol content, antioxidant and anti-acetylcholinesterase activities, and impact of exposure to simulated gastrointestinal fluids. Antioxidants 5(2):12
13. Matilla P, Astola J, Kumpulanien J (2000) Determination of flavonoids in plant material by HPLC with diode-array and electro-array detections. J Food Chem 48:5834–5841
14. Seikel MK (1962) Chromatographic methods of separation, isolation and identification of flavonoid compounds. In: Geissman TA (ed) The chemistry of flavonoid compounds. Macmillan Co., New York, p 34

15. Rahman MM, Islam MB, Biswas M, Khurshid Alam AH (2015) In vitro antioxidant and free radical scavenging activity of different parts of Tabebuia pallida growing in Bangladesh. BMC Res Notes 8:621–628
16. Arnao MB, Cano A, Acosta M (2001) The hydrophilic and lipophilic contribution to total antioxidant activity. Food Chem 73:239–244
17. Alaa AM, El-Azab AS, Abou-Zeid LA, ElTahir KE, Abdel-Aziz NI, Ayyad RR, Al-Obaid AM (2016) Synthesis, anti-inflammatory, analgesic and COX-1/2 inhibition activities of anilides based on 5, 5-diphenylimidazolidine-2, 4-dione scaffold: molecular docking studies. Eur J Med Chem 115:121–131
18. Huang Y, Zhang B, Li J, Liu H, Zhang Y, Yang Z, Liu W (2019) Design, synthesis, biological evaluation and docking study of novel indole-2-amide as anti-inflammatory agents with dual inhibition of COX and 5-LOX. Eur J Med Chem 180:41–50
19. Harman CA, Turman MV, Kozak KR, Marnett LJ, Smith WL, Garavito RM (2007) Structural basis of enantioselective inhibition of cyclooxygenase-1 by S-α-substituted indomethacin ethanolamides. J Biol Chem 282(38):28096–28105
20. Pettersen EF, Goddard TD, Huang CC, Couch GS, Greenblatt DM, Meng EC, Ferrin TE (2004) UCSF Chimera—a visualization system for exploratory research and analysis. J Comput Chem 25(13):1605–1612
21. Li H, Robertson AD, Jensen JH (2005) Very fast empirical prediction and rationalization of protein pKa values. Proteins 61:704–721
22. Halford B (2014) Reflections on ChemDraw. Chem Eng News Arch 92:26–27
23. Hanwell MD, Curtis DE, Lonie DC, Vandermeersch T, Zurek E, Hutchison GR (2012) Avogadro: an advanced semantic chemical editor, visualization, and analysis platform. J Cheminform 4(1):1–7
24. Trott O, Olson AJ (2010) AutoDock Vina: improving the speed and accuracy of docking with a new scoring function, efficient optimization, and multithreading. J Comput Chem 31:455–461
25. Bikadi Z, Hazai E (2009) Application of the PM6 semi-empirical method to modeling proteins enhances docking accuracy of AutoDock. J Cheminform 1:1–16
26. Huey R, Morris GM (2006) Using autodock with autodocktools: a tutorial. The Scripps Research Institute Molecular Graphics Laboratory, California
27. Morris GM, Goodsell DS, Halliday RS, Huey R, Hart WE, Belew RK, Olson AJ (1998) Automated docking using a Lamarckian genetic algorithm and an empirical binding free energy function. J Comput Chem 19(14):1639–1662
28. Hospital A, Goñi JR, Orozco M, Gelpí JL (2015) Molecular dynamics simulations: advances and applications. Adv Appl Bioinform Chem 8:37–47
29. Mirzaei S, Eisvand F, Hadizadeh F, Mosaffa F, Ghasemi A, Ghodsi R (2020) Design, synthesis and biological evaluation of novel 5,6,7-trimethoxy-N-aryl-2-styrylquinolin-4-amines as potential anticancer agents and tubulin polymerization inhibitors. Bioorg Chem 98:103711
30. Hasanin M, Hashem AH, El-Rashedy AA, Kamel S (2021) Synthesis of novel heterocyclic compounds based on dialdehyde cellulose: characterization, antimicrobial, antitumor activity, molecular dynamics simulation and target identification. Cellulose 28:8355–8374
31. Roe DR, Cheatham TE III (2013) PTRAJ and CPPTRAJ: software for processing and analysis of molecular dynamics trajectory data. J Chem Theory Comput 9(7):3084–3095
32. Seifert E (2014) OriginPro 9.1: scientific data analysis and graphing software—software review. J Chem Inf Model 54:1552–1552
33. Kollman PA, Massova I, Reyes C, Kuhn B, Huo S, Chong L, Lee M, Lee T, Duan Y, Wang W, Donini O (2000) Calculating structures and free energies of complex molecules: combining molecular mechanics and continuum models. Acc Chem Res 33(12):889–897
34. Ylilauri M, Pentikäinen OT (2013) MMGBSA as a tool to understand the binding affinities of filamin-peptide interactions. J Chem Inf Model 53:2626–2633
35. Hayes JM, Archontis G (2012) MM-GB(PB)SA calculations of protein-ligand binding free energies. In: Molecular dynamics—studies of synthetic and biological macromolecules, vol 11, pp 171–190
36. Choi JM, Lee EO, Lee HJ, Kim KH, Ahn KS, Shim BS, Kim NI, Song MC, Baek NI, Kim SH (2007) Identification of Campesterol from *Chrysanthemum coronarium* L. and its antiangiogenic activities. Phytother Res 21:954–959
37. Jain PS, Bari SB (2010) Isolation of lupeol, stigmasterol and campesterol from petroleum ether extract of woody stem of *Wrightia tinctoria*. Asian J Plant Sci 9:163–167
38. Musa WJ, Duengo S, Kilo AK (2019) Campesterol from methanol fraction of brotowali (tinospora crispa) stem bark. Comp Lit 11:95–97
39. Ghosh K, Bhattacharya TK (2005) Chemical constituents of *Piper betle* Linn. (Piperaceae) roots. Molecules 10:798–802
40. Udobre AS, Etim EI, Udobang JA, Udoh AE (2015) Antimicrobial activity of stigmast-4-en-3-one and 2,4-dimethylhexane isolated from nauclea latifolia. Int J Phytopharm Res 6(2):65–68
41. Aboulthana WM, Youssef A, El-Feky AM, El-Sayed NI, Seif MM, Hassan AK (2019) Evaluation of antioxidant efficiency of Croton tiglium L. seeds extracts after incorporating silver nanoparticles. Egypt J Chem 62(2):181–200
42. Horník Š, Sajfrtová M, Karban J, Sýkora J, Březinová A, Wimmer Z (2013) LC-NMR technique in the analysis of phytosterols in natural extracts. J Anal Methods Chem 2013:1–9
43. Eswaraiah MC, Elumalai A (2011) Isolation of phytoconstituents from the stems of Mussaenda erythrophylla. Pharm Sin 2:132–142
44. Shrestha A, Pandey RP, Dhakal D, Parajuli P, Sohng JK (2018) Biosynthesis of flavone C-glucosides in engineered *Escherichia coli*. Appl Microbiol Biotechnol 102:1251–1267
45. Kutil Z, Temml V, Maghradze D, Pribylova M, Dvorakova M, Schuster D, Vanek T, Landa P (2014) Impact of wines and wine constituents on cyclooxygenase-1, cyclooxygenase-2, and 5-lipoxygenase catalytic activity. Mediat Inflamm 2014:1–8
46. Kaur G, Silakari O (2017) Multiple target-centric strategy to tame inflammation. Future Med Chem 9:1361–1376
47. Awaad AS, El-Meligy RM, Soliman GA (2013) Natural products in treatment of ulcerative colitis and peptic ulcer. J Saudi Chem Soc 17:101–124
48. Courts FL, Williamson G (2015) The occurrence, fate and biological activities of C-glycosyl flavonoids in the human diet. Crit Rev Food Sci Nutr 55(10):1352–1367
49. Roy A, Khan A, Ahmad I, Alghamdi S, Rajab BS, Babalghith AO, Alshahrani MY, Islam S, Islam M (2022) Flavonoids a bioactive compound from medicinal plants and its therapeutic applications. Biomed Res Int 2022:1–9
50. Yoshida Y, Niki E (2003) Antioxidant effects of phytosterol and its components. J Nutr Sci Vitaminol 49(4):277–280
51. Dias MC, Pinto DC, Silva AM (2021) Plant flavonoids: chemical characteristics and biological activity. Molecules 26(17):5377
52. Ullah A, Munir S, Badshah SL, Khan N, Ghani L, Poulson BG, Emwas AH, Jaremko M (2020) Important flavonoids and their role as a therapeutic agent. Molecules 25(22):5243
53. Salehi B, Quispe C, Sharifi-Rad J, Cruz-Martins N, Nigam M, Mishra AP, Konovalov DA, Orobinskaya V, Abu-Reidah IM, Zam W, Sharopov F (2021) Phytosterols: from preclinical evidence to potential clinical applications. Front Pharmacol 11:599959
54. Machaba KE, Mhlongo NN, Soliman MES (2018) Induced mutation proves a potential target for TB therapy: a molecular dynamics study on LprG. Cell Biochem Biophys 76:345–356
55. Pan L, Patterson JC, Deshpande A, Cole G, Frautschy S (2013) Molecular dynamics study of Zn(Aβ) and Zn(Aβ)2. PLoS ONE 8:70681–70688
56. Wijffels G, Dalrymple B, Kongsuwan K, Dixon N (2005) Conservation of eubacterial replicases. IUBMB Life 57:413–419
57. Richmond TJ (1984) Solvent accessible surface area and excluded volume in proteins: analytical equations for overlapping spheres and implications for the hydrophobic effect. J Mol Biol 178:63–89
58. Cournia Z, Allen B, Sherman W (2017) Relative binding free energy calculations in drug discovery: recent advances and practical considerations. J Chem Inf Model 57:2911–2937
59. Nassar AEF, Kamel AM, Clarimont C (2004) Improving the decision-making process in the structural modification of drug candidates: enhancing metabolic stability. Drug Discov Today 9:1020–1028
60. Pairet M, Engelhardt G (1996) Distinct isoforms (COX-1 and COX-2) of cyclooxygenase: possible physiological and therapeutic implications. Fundam Clin Pharmacol 10:1–15
61. Assumpção TCF, Alvarenga PH, Ribeiro JMC, Andersen JF, Francischetti IMB (2010) Dipetalodipin, a novel multifunctional salivary lipocalin that inhibits platelet aggregation, vasoconstriction, and angiogenesis through

unique binding specificity for TXA2, PGF2alpha, and 15(S)-HETE. J Biol Chem 285:39001–39012
62. Innes JK, Calder PC (2018) Omega-6 fatty acids and inflammation. Prostaglandins Leukot Essent Fatty Acids 132:41–48

Publisher's Note